PHOTONICS Research

Bistable lasing in parity-time symmetric coupled fiber rings

Sergey V. Smirnov,[1,*] Maxim O. Makarenko,[1] Sergey V. Suchkov,[2] Dmitry Churkin,[1] and Andrey A. Sukhorukov[2]

[1]Novosibirsk State University, 2 Pirogova Street, Novosibirsk 630090, Russia
[2]Nonlinear Physics Centre, Research School of Physics and Engineering, Australian National University, Canberra, ACT 2601, Australia
*Corresponding author: smirnov@lab.nsu.ru

Received 20 September 2017; accepted 12 January 2018; posted 12 January 2018 (Doc. ID 307530); published 20 March 2018

We propose a parity-time (PT) symmetric fiber laser composed of two coupled ring cavities with gains and losses, which operates both in PT-symmetric and symmetry-broken regimes depending on the static phase shifts. We perform analytical and numerical analysis by the transfer matrix method taking into account gain saturation and predict laser bistability in the PT-symmetric regime in contrast to a symmetry-broken single-mode operation. In the PT-broken regime, the generation power counterintuitively increases with an increase of the cavity losses.

OCIS codes: (060.3510) Lasers, fiber; (190.1450) Bistability; (140.3560) Lasers, ring.

https://doi.org/10.1364/PRJ.6.000A18

1. INTRODUCTION

The concept of parity-time (PT) symmetry in optics has attracted a great deal of attention following the first experimental demonstrations only a few years ago [1,2]. It suggests new prospects for the design of optical structures with symmetrically distributed regions of gain and losses; see review papers [3–5] and references therein.

Recently, PT-symmetric lasers were demonstrated experimentally in microrings [6–9]. Importantly, a single-mode laser operation was achieved in an initially multi-mode system through stronger mode discrimination, when the system operates in the PT-broken regime close to a PT-symmetry-breaking transition. Also, a single transverse-mode operation in a system of coupled microring lasers was demonstrated near the exceptional point [10], and enhanced sensitivity [11,12] was realized. In a pair of coupled microdisk quantum cascade lasers, the reversal of generated power dependence [13] was identified in the vicinity of exceptional points (EPs), where spontaneous emission is enhanced [14], and EPs were observed directly in photonic-crystal lasers [15]. Furthermore, a realization of PT-symmetry-based mode locking [16] and a PT-symmetric laser absorber [17] were theoretically proposed, and lasing and anti-lasing in a single cavity were demonstrated [18]. Recently, a statistical PT-symmetric lasing has been achieved in an optical fiber network incorporating semiconductor amplifiers [19].

In this work, we develop the theoretical concept of a PT-symmetric fiber laser based on coupled cavities. We use a conventional ring cavity laser design and predict PT-symmetric and PT-broken lasing by means of tunable coupling of a ring cavity laser with a passive cavity.

2. METHODS AND RESULTS

We present a diagram of the proposed PT-symmetric fiber ring laser in Fig. 1. The scheme comprises two similar fiber cavities: one of them is active (with gain), and the other cavity is passive (with losses). Tunable coupling between cavities is controlled by means of adjustable phase shifts inside a Mach–Zehnder interferometer. In the case of zero phase shifts, passive and active cavities are uncoupled, so the system acts as a conventional ring cavity laser if properly pumped. As we demonstrate below, tunable coupling enables one to switch between PT-symmetric and PT-broken lasing regimes.

To describe the laser operation and associated PT transitions, we use a discrete transfer matrix model governing the evolution of the field amplitudes in both fiber cavities. Field evolution over a cavity round-trip in the first approximation is described by a transfer operator $\boldsymbol{L}$,

$$\boldsymbol{L}=\begin{pmatrix} e^{g_1/2} & 0 \\ 0 & e^{g_2/2} \end{pmatrix}\begin{pmatrix} 0 & 1 \\ 1 & 0 \end{pmatrix}\begin{pmatrix} 1/\sqrt{2} & i/\sqrt{2} \\ i/\sqrt{2} & 1/\sqrt{2} \end{pmatrix} \times \begin{pmatrix} e^{i\varphi_1} & 0 \\ 0 & e^{i\varphi_2} \end{pmatrix}\begin{pmatrix} 1/\sqrt{2} & i/\sqrt{2} \\ i/\sqrt{2} & 1/\sqrt{2} \end{pmatrix}\begin{pmatrix} e^{g_1/2} & 0 \\ 0 & e^{g_2/2} \end{pmatrix}, \quad (1)$$

where $g_2 < 0$ denotes constant losses and $g_1 > 0$ characterizes total gain. Importantly, crossover coupling as described by the second matrix in Eq. (1) facilitates PT symmetry with static

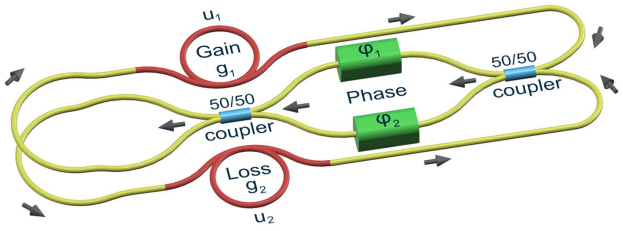

Fig. 1. Schematic of the proposed PT-symmetric fiber-ring laser, composed of two coupled fiber-ring cavities with gain and losses. The coupling between cavities is controlled by means of phase shifts φ_1 and φ_2. Arrows indicate the direction of propagation.

elements, whereas active modulation was required in previous realizations of mesh lattices [20].

We simplify Eq. (1) and express the operator as

$$\boldsymbol{L} = ie^{\tilde{g}+i\tilde{\varphi}}\begin{pmatrix} e^{\Delta g/2}\cos\left(\frac{\Delta\varphi}{2}\right) & -\sin\left(\frac{\Delta\varphi}{2}\right) \\ \sin\left(\frac{\Delta\varphi}{2}\right) & e^{-\Delta g/2}\cos\left(\frac{\Delta\varphi}{2}\right) \end{pmatrix}, \tag{2}$$

where $\tilde{g} \equiv (g_1 + g_2)/2$, $\Delta g \equiv g_1 - g_2$, $\tilde{\varphi} \equiv (\varphi_1 + \varphi_2)/2$, and $\Delta\varphi \equiv \varphi_1 - \varphi_2$. Note that $\Delta\varphi = 0$ corresponds to uncoupled cavities, whereas $\Delta\varphi = \pi$ means completely cross-coupled cavities.

We establish that the operator $\boldsymbol{L}$ possesses PT symmetry when applied in conjunction with the Gauge transformation,

$$\boldsymbol{PT}e^{-\tilde{g}-i\tilde{\varphi}}\boldsymbol{L} = e^{-\tilde{g}-i\tilde{\varphi}}\boldsymbol{LPT}. \tag{3}$$

The parity operator swaps the two fibers,

$$\boldsymbol{P} = \begin{pmatrix} 0 & 1 \\ 1 & 0 \end{pmatrix}, \tag{4}$$

which effectively interchanges the gain and phase coefficients since

$$\boldsymbol{PL}(g_1, g_2, \varphi_1, \varphi_2)\boldsymbol{P}^{-1} = \boldsymbol{L}(g_2, g_1, \varphi_2, \varphi_1). \tag{5}$$

The time-reversal operator $\boldsymbol{T}$ performs complex conjugation and also swaps the propagation direction,

$$\boldsymbol{TL} = (\boldsymbol{L}^*)^{-1}\boldsymbol{T}. \tag{6}$$

The signal propagation through the considered system can be fully described by the eigenvalues $\mu_\pm$ and eigenvectors $(u_1, u_2)^{\mathrm{T}}$ of the operator $\boldsymbol{L}$, which are found as

$$\begin{aligned} \mu_\pm &= ie^{\tilde{g}+i\tilde{\varphi}}\tilde{\mu}_\pm, \\ \tilde{\mu}_\pm &= 1/\tilde{\mu}_\mp = \cosh(\Delta g/2)\cos(\Delta\varphi/2) \\ &\quad \pm \sqrt{\cosh^2(\Delta g/2)\cos^2(\Delta\varphi/2) - 1} \end{aligned} \tag{7}$$

and

$$\begin{pmatrix} u_1 \\ u_2 \end{pmatrix} = \begin{pmatrix} \exp(i\nu_\pm/2) \\ \exp(-i\nu_\pm/2) \end{pmatrix}, \tag{8}$$

where

$$\nu_\pm = -i\log\left[\frac{\tilde{\mu}_\pm - e^{-\Delta g/2}\cos\left(\frac{\Delta\varphi}{2}\right)}{\sin\left(\frac{\Delta\varphi}{2}\right)}\right]. \tag{9}$$

We note that there is an exceptional point where the two eigenvalues become identical ($\mu_+ = \mu_-$) when the gain/losses difference reaches a value

$$\Delta g_{\mathrm{PT}} = 2\cosh^{-1}\left[\frac{1}{\cos(\Delta\varphi/2)}\right], \tag{10}$$

which corresponds to the PT-symmetry-breaking threshold when $\tilde{g} = 0$.

We present in Fig. 2(a) the ratio of two eigenvalues, $|\mu_+/\mu_-|$, and in Fig. 2(b) the relative phase of the mode amplitudes, $\arg(u_1/u_2)|_{\mu_+} = \mathrm{Re}(\nu_+)$, versus the difference of phases and gain/loss in two fiber-ring cavities.

The modes are in the PT-symmetric regime for $|\Delta g| < \Delta g_{\mathrm{PT}}$. In this case, $\mathrm{Im}(\nu_\pm) = 0$ and

$$\nu_+ = -\nu_-, \tag{11}$$

and accordingly the eigenmode intensities are equal in the active and passive cavities, $|u_1| = |u_2|$. Thus, both modes exhibit the same amplification or absorption averaged over two fiber cavities, $|\mu_+| = |\mu_-| = \exp(\tilde{g})$. Note that PT symmetry always holds for $\Delta\varphi = \pm\pi$, when the fiber cavities are completely cross-coupled, such that the optical path goes through both active and passive cavities and the influences of gain and losses are compensated.

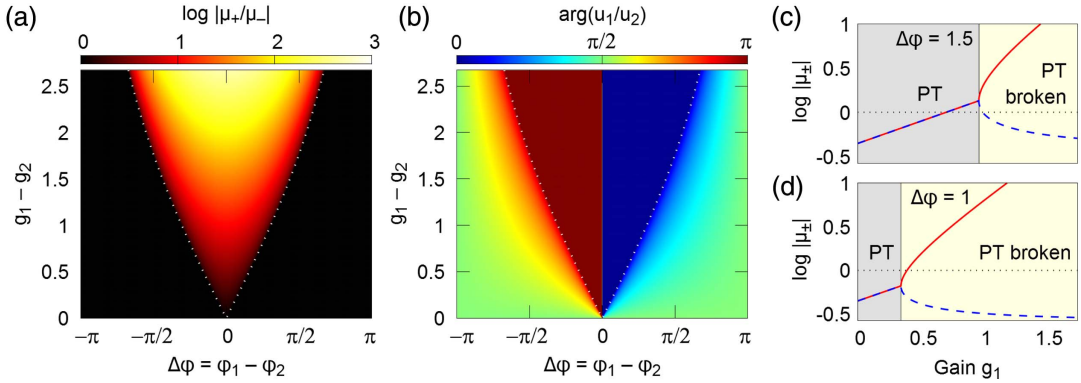

Fig. 2. (a) Ratio of two linear mode eigenvalues, $|\mu_+/\mu_-|$ and (b) the relative phase of the eigenmode amplitudes $\arg(u_1/u_2)_{\mu_+} = \mathrm{Re}(\nu_+)$ versus the difference of phases and gain/losses in two fiber cavities. White dotted lines indicate the PT-breaking boundary. (c), (d) The absolute eigenvalues shown with solid ($|\mu_+|$) and dashed ($|\mu_-|$) lines versus the gain coefficient for fixed losses ($g_2 = -0.7$) and different phases (c) $\Delta\varphi = 1.5$ and (d) $\Delta\varphi = 1$. Horizontal dotted line marks the level $|\mu| = 1$ corresponding to stationary modes with balanced gain and losses.

In the PT-broken regime when $|\Delta g| > \Delta g_{PT}$, the modes exhibit a different rate of amplification or absorption with $|\mu_+| > |\mu_-|$, while $\nu_\pm$ are purely imaginary, and accordingly, the amplitudes $u_{1,2}$ are exactly in or out of phase. We note that the PT-broken regime is always realized for $\Delta\varphi = 0$, since in this case the cavities become effectively uncoupled, so the mode in the active cavity experiences amplification, while the mode in the passive cavity attenuates.

We plot in Figs. 2(c) and 2(d) the characteristic dependencies of the eigenvalues on the gain coefficient g_1, while keeping losses fixed ($g_2 < 0$). For a phase detuning such that

$$\cos(\Delta\varphi/2) < 1/\cosh(|g_2|), \tag{12}$$

the net amplification regime is realized at $g_1 > |g_2|$ simultaneously for two eigenmodes in the PT-symmetric regime [$|\mu_\pm| = \exp(\tilde{g}) > 1$], whereas PT breaking occurs at stronger gain after the bifurcation at the exceptional point; see Fig. 2(c). On the other hand, for the phase detunings with

$$\cos(\Delta\varphi/2) > 1/\cosh(|g_2|) \tag{13}$$

in the PT-symmetric regime, both modes are attenuated on average [$|\mu_\pm| = \exp(\tilde{g}) < 1$], while net amplification is achieved for one mode at stronger gain in the PT-broken regime ($|\mu_+| > 1$); see Fig. 2(d).

Essentially, the model with a constant gain as represented above describes an amplifier operating in the regime of small signal gain, not a laser. The laser is characterized by self-governing gain saturation that limits the total gain over the round trip to be equal to total round-trip losses [21]. In the following, we consider a simple model of gain saturation,

$$g_1 = \frac{g_0}{1 + \tilde{P}_1} - g_h, \tag{14}$$

where $\tilde{P}_1$ is the normalized power at the input of the gain element in the current round trip. According to Eq. (14), the gain element introduces losses ($-g_h < 0$) at a high power level, whereas its amplification of weak field is $g_0 - g_h$.

For lasing to occur, small-amplitude fields need to be amplified, i.e., it is necessary to have $|\mu_+|_{\tilde{P}_1=0} > 1$. Then, the optical power will grow with each fiber cavity round trip until the gain gets saturated and a stationary regime is reached where gain and losses are exactly balanced, $|\mu_+|_{\tilde{P}_1} = 1$. The latter condition corresponds to a transition from net losses to a net gain for varying gain strength (g_1), which can be satisfied in PT-symmetric or PT-broken regime depending on parameters, as we have illustrated above in Figs. 2(b) and 2(c). Specifically, PT-symmetric lasing can occur for phases satisfying Eq. (12) above a critical gain $g_0 - g_h > |g_2|$. On the other hand, the PT-broken regime occurs at a lower gain threshold for a range of phases defined in Eq. (13). We summarize the different parameter domains and gain thresholds for possible laser regimes in Fig. 3(a).

A characteristic dependence of mode amplification on power in the PT-symmetric laser regime is presented in Fig. 3(b). We see that although PT symmetry is broken at low powers, it is restored at higher powers, when gain is effectively reduced due to saturation. A stationary lasing regime at exactly balanced gain and losses, i.e., when $|\mu_\pm| = 1$, can be achieved both in PT (closed circle) and PT-broken (open circle) regimes. The open circle corresponds to the unstable regime, due to co-existence of another mode which exhibits net amplification. Conversely, a closed circle marks a stationary state, which can be realized simultaneously for both PT-symmetric modes. We show in the following that this leads to bi-stability in a laser operation. On the other hand, in the PT-broken laser regime, a stationary stable point appears only for one mode, as illustrated in Fig. 3(c).

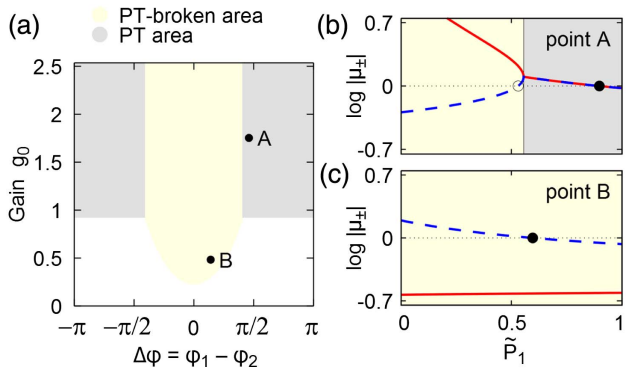

Fig. 3. (a) Stationary regimes of laser operation with nonlinear gain saturation: no lasing (white background), pair of PT-symmetric laser modes (grey shading), or one mode in PT-broken regime (yellow shading). (b), (c) Characteristic mode amplification versus power for points A and B marked in (a) corresponding to different lasing regimes. Solid circles mark stable and the open circle marks unstable regimes with balanced gain and loss (zero mode amplification). Background shading marks PT-symmetric and broken regimes. Saturable gain parameter $g_h = 0.23$ (1 dB).

Measurements of eigenvalues in a real laser are not straightforward. The most direct way to characterize the PT transition is to measure generated powers in both active and passive fiber cavities, $P_1 = |u_1|^2$ and $P_2 = |u_2|^2$, respectively. As we have discussed above, in the PT-symmetric regime $P_1 = P_2$, whereas in the PT-broken case $P_1 > P_2$. Thus the most straightforward way to identify whether the system operates in PT-symmetric or PT-broken phases is to measure power ratio P_2/P_1. We plot its predicted dependence in Fig. 4(a) as a

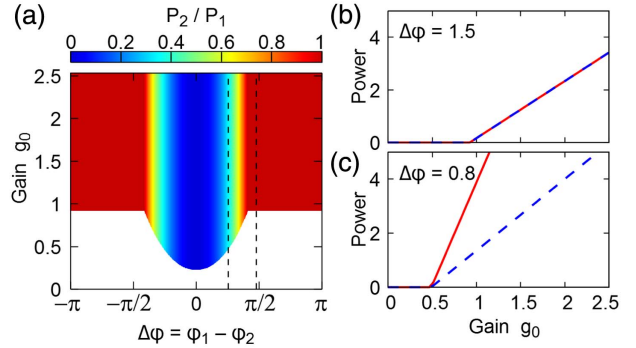

Fig. 4. Power dependencies in stationary lasing regimes. (a) A ratio of power generated in passive and active cavities, P_2/P_1, is unity in PT-symmetrical region and less than unity in PT-broken area. (b), (c) Dependence of the lasing power in two cavities on the gain in PT-symmetric and PT-broken regimes corresponding to different phase shift $\Delta\varphi = 1.5$ and 0.8, respectively, both shown with dashed lines in plot (a).

function of gain coefficient (i.e., the amount of pumping in the active cavity) and the phase shift (i.e., amount of coupling). We emphasize that the generation threshold of the laser is a function of the phase shift in the PT-broken case, whereas in the PT-symmetrical area the threshold does not depend on the phase shift. We illustrate a characteristic dependence of the lasing power in two cavities on the gain in PT-symmetric and PT-broken regimes in Figs. 4(b) and 4(c), respectively. We see that for any gain level, in the PT-symmetric case the generated powers are equal in both cavities ($P_2/P_1 = 1$), although only the active one is pumped. In the PT-broken case, the power in the passive cavity is always less compared to the power generated in the active cavity, i.e., $P_2/P_1 < 1$. In particular, in the limiting case of uncoupled cavities (zero phase shift $\Delta\varphi = 0$), the power in the passive cavity is completely zero, yielding $P_2/P_1 = 0$.

In a conventional laser, the higher the optical losses, the less is a generation power. We find that this is not always the case in a considered system of fiber laser with a PT symmetry. Indeed, when optical losses g_2 are varied, lasing power P_1 changes in a complex way; see Fig. 5(a). In a PT-symmetric area, the higher the losses $|g_2|$, the lower the lasing power, whereas in the PT-broken area lasing power P_1 grows with the increase of the optical losses $|g_2|$. Correspondingly, there are three scenarios of the dependence of lasing power P_1 on losses g_2, defined by the relative positions of PT symmetric, PT-broken, and under-threshold areas. Thus, at relatively small $\Delta\varphi$, i.e., in the case of weakly coupled cavities, areas of PT-symmetric and PT-broken solutions are adjacent [see Fig. 5(b)], so that lasing power P_1 drops to its minimum value and then grows in the PT-broken area while cavity losses are increased. At larger phase shifts $\Delta\varphi$, there is a gap between PT-symmetric and PT-broken areas where the laser is under threshold; see Fig. 5(c). Finally, at large phase shifts $\Delta\varphi$, i.e., in the case of strongly coupled cavities, the PT-broken area disappears and lasing power drops monotonically down to zero in the PT area while optical losses are increased; see Fig. 5(d). We note that an increase of lasing power P_1 along with optical losses $|g_2|$ appears as a result of energy redistribution between cavities, rather than the total energy growth. A conceptually similar power dependence has been reported recently in a PT laser of another type [19].

We now analyze how the laser reaches its stationary state, i.e., the laser dynamics. To establish the general dynamical properties, we study the evolution of the following quantity:

$$J = \mathrm{Im}(u_1 u_2^*) = |u_1 u_2| \sin[\arg(u_1) - \arg(u_2)]. \tag{15}$$

Considering complex amplitudes u_1 and u_2, we find that after the evolution over one period described by matrix $\boldsymbol{L}$ with arbitrary phase and gain coefficients in Eq. (2),

$$J \to e^{2\tilde{g}} J. \tag{16}$$

Thus, the following quantity remains invariant during evolution, both in PT and PT-broken regimes:

$$\mathrm{sign}(J) = \mathrm{sign}\{\sin[\arg(u_1) - \arg(u_2)]\} = \mathrm{const}. \tag{17}$$

Accordingly, the relative phase is confined to one of two domains, depending on the initial conditions,

$$\begin{aligned} 0 &< \arg(u_1) - \arg(u_2) < \pi, \\ -\pi &< \arg(u_1) - \arg(u_2) < 0. \end{aligned} \tag{18}$$

We show these regions with different shadings in Fig. 6(a). We also indicate with solid and dashed lines possible stationary lasing states, which could be realized for various structural parameters.

The horizontal lines with $\arg(u_1) - \arg(u_2) = \{0, \pm\pi\}$ in Fig. 6(a) correspond to stationary PT-broken modes, according to the general features discussed above. Importantly, PT-broken states appear at the boundaries of two phase regions determined in Eq. (18), and therefore for any input state the laser can converge to a single PT-broken lasing mode operation.

Stationary PT-symmetric modes can appear along the vertical lines at $|P_2/P_1| = 1$, as indicated in Fig. 6(a). The pairs of PT-symmetric modes have opposite relative phases according to Eq. (11), and therefore they necessarily appear inside distinct regions; see an example of two modes corresponding to particular structure parameters marked with black circles in Fig. 6(a). This indicates a bi-stable laser operation, since each of the stationary points can act as an attractor for all initial states inside the associated phase region, while the boundary between these regions cannot be crossed. We illustrate the bi-stable dynamics in Figs. 6(b) and 6(c), which show that depending on initial phase difference between the amplitudes in two fiber cavities (but not on initial powers), the laser converges either to the first or second PT-symmetric eigenmode.

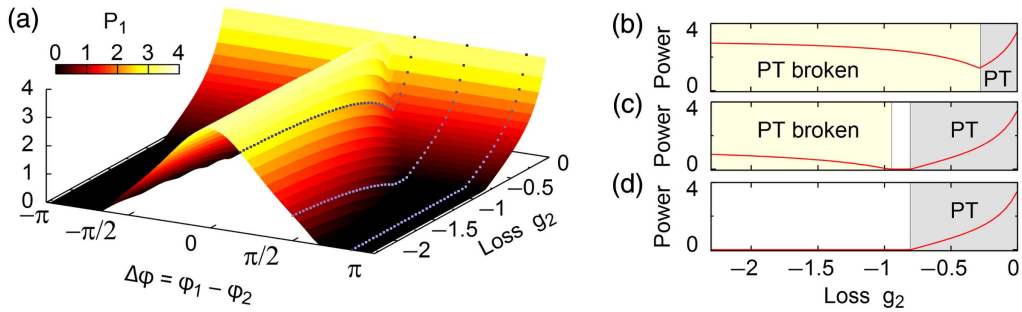

Fig. 5. (a) Dependence of generated power P_1 on phase shift $\Delta\varphi$ and loss g_2 at fixed gain $g_1 = 1.0$ has non-trivial form resulting from PT transition. In the PT-symmetric area, the higher are the losses $|g_2|$, the lower is the lasing power as it should be in a conventional laser, whereas in the case of PT-broken regime, the generation power increases with the increase of losses. Panels (b)–(d) are cross sections of a 3D surface indicated on panel (a) over dotted lines.

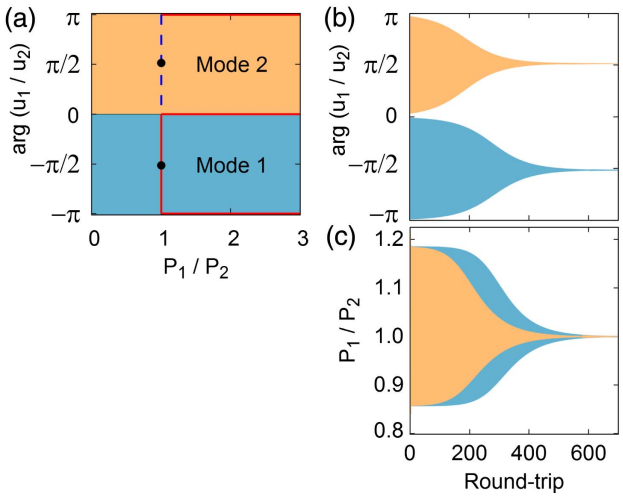

Fig. 6. Dynamical properties of a PT-symmetric fiber laser. (a) Two trapping regions shown with shading according to Eq. (18), shown in the plane of relative phases and powers in two fiber cavities. Laser dynamics is confined to one region according to the initial conditions. Solid and dashed lines indicate possible stationary lasing states: PT-symmetric—vertical lines at $P_2/P_1 = 1$, and PT-broken—horizontal lines at relative phases $\{0, \pm\pi\}$. (b), (c) Dynamical evolution demonstrating bi-stability on the PT-symmetric regime. Shown are relative (b) phases and (c) powers, which converge to one of two stationary states marked with solid circles in (a). Parameters are $g_1 = 2.3$, $g_2 = -0.7$, and $\Delta\varphi = 2.95$.

3. CONCLUSION

In conclusion, we proposed and analyzed theoretically a PT-symmetric fiber-ring laser composed of two active and passive cavities with a cross-coupling element, which allows us to switch between PT-symmetric and broken regimes without using active modulation of gain/loss elements. We considered the effect of gain saturation at high powers and predicted that the system always converges to a stationary lasing state, while demonstrating bi-stable behavior in the PT-symmetric regime. We also revealed that the generated power nontrivially depends on the optical losses, as in PT-broken regime the lasing power increases for stronger losses, whereas lasing can be completely suppressed for intermediate loss levels between the PT-symmetric and PT-broken regions.

Funding. Russian Science Foundation (RSF) (16-12-10402); Australian Research Council (ARC) (DP160100619).

Acknowledgment. This work was supported by the Russian Science Foundation. S. V. Suchkov and A. A. Sukhorukov are supported by the Australian Research Council.

REFERENCES

1. A. Guo, G. J. Salamo, D. Duchesne, R. Morandotti, M. Volatier-Ravat, V. Aimez, G. A. Siviloglou, and D. N. Christodoulides, "Observation of PT-symmetry breaking in complex optical potentials," Phys. Rev. Lett. **103**, 093902 (2009).
2. C. E. Ruter, K. G. Makris, R. El Ganainy, D. N. Christodoulides, M. Segev, and D. Kip, "Observation of parity-time symmetry in optics," Nat. Phys. **6**, 192–195 (2010).
3. A. A. Zyablovsky, A. P. Vinogradov, A. A. Pukhov, A. V. Dorofeenko, and A. A. Lisyansky, "PT-symmetry in optics," Phys. Usp. **57**, 1063–1082 (2014).
4. V. V. Konotop, J. K. Yang, and D. A. Zezyulin, "Nonlinear waves in PT-symmetric systems," Rev. Mod. Phys. **88**, 035002 (2016).
5. S. V. Suchkov, A. A. Sukhorukov, J. H. Huang, S. V. Dmitriev, C. Lee, and Y. S. Kivshar, "Nonlinear switching and solitons in PT-symmetric photonic systems," Laser Photon. Rev. **10**, 177–213 (2016).
6. L. Feng, Z. J. Wong, R. M. Ma, Y. Wang, and X. Zhang, "Single-mode laser by parity-time symmetry breaking," Science **346**, 972–975 (2014).
7. H. Hodaei, M. A. Miri, M. Heinrich, D. N. Christodoulides, and M. Khajavikhan, "Parity-time-symmetric microring lasers," Science **346**, 975–978 (2014).
8. H. Hodaei, A. U. Hassan, W. E. Hayenga, M. A. Miri, D. N. Christodoulides, and M. Khajavikhan, "Dark-state lasers: mode management using exceptional points," Opt. Lett. **41**, 3049–3052 (2016).
9. W. L. Liu, M. Li, R. S. Guzzon, E. J. Norberg, J. S. Parker, M. Z. Lu, L. A. Coldren, and J. P. Yao, "An integrated parity-time symmetric wavelength-tunable single-mode microring laser," Nat. Commun. **8**, 15389 (2017).
10. H. Hodaei, M. A. Miri, A. U. Hassan, W. E. Hayenga, M. Heinrich, D. N. Christodoulides, and M. Khajavikhan, "Single mode lasing in transversely multi-moded PT-symmetric microring resonators," Laser Photon. Rev. **10**, 494–499 (2016).
11. J. Ren, H. Hodaei, G. Harari, A. U. Hassan, W. Chow, M. Soltani, D. Christodoulides, and M. Khajavikhan, "Ultrasensitive micro-scale parity-time-symmetric ring laser gyroscope," Opt. Lett. **42**, 1556–1559 (2017).
12. H. Hodaei, A. U. Hassan, S. Wittek, H. Garcia-Gracia, R. El Ganainy, D. N. Christodoulides, and M. Khajavikhan, "Enhanced sensitivity at higher-order exceptional points," Nature **548**, 187–191 (2017).
13. M. Brandstetter, M. Liertzer, C. Deutsch, P. Klang, J. Schoberl, H. E. Tureci, G. Strasser, K. Unterrainer, and S. Rotter, "Reversing the pump dependence of a laser at an exceptional point," Nat. Commun. **5**, 4034 (2014).
14. A. Pick, B. Zhen, O. D. Miller, C. W. Hsu, F. Hernandez, A. W. Rodriguez, M. Soljacic, and S. G. Johnson, "General theory of spontaneous emission near exceptional points," Opt. Express **25**, 12325–12348 (2017).
15. K. H. Kim, M. S. Hwang, H. R. Kim, J. H. Choi, Y. S. No, and H. G. Park, "Direct observation of exceptional points in coupled photonic-crystal lasers with asymmetric optical gains," Nat. Commun. **7**, 13893 (2016).
16. S. Longhi, "PT-symmetric mode-locking," Opt. Lett. **41**, 4518–4521 (2016).
17. S. Longhi, "PT-symmetric laser absorber," Phys. Rev. A **82**, 031801 (2010).
18. Z. J. Wong, Y. L. Xu, J. Kim, K. O'Brien, Y. Wang, L. Feng, and X. Zhang, "Lasing and anti-lasing in a single cavity," Nat. Photonics **10**, 796–801 (2016).
19. A. K. Jahromi, A. U. Hassan, D. Christodoulides, and A. Abouraddy, "Statistical parity-time-symmetric lasing in an optical fiber network," Nat. Commun. **8**, 1359 (2017).
20. A. Regensburger, C. Bersch, M. A. Miri, G. Onishchukov, D. N. Christodoulides, and U. Peschel, "Parity-time synthetic photonic lattices," Nature **488**, 167–171 (2012).
21. L. Ge and R. El Ganainy, "Nonlinear modal interactions in parity-time (PT) symmetric lasers," Sci. Rep. **6**, 24889 (2016).